Supporting Information

Dual sensing of fluoride ions by *o*-carborane–triarylborane dyad

Ki Cheol Song,[a] *Hyungjun Kim,*[a] *Kang Mun Lee,*[a] *Yoon Sup Lee,*[a] *Youngkyu Do**[a] *and Min Hyung Lee**[b]

[a] Department of Chemistry, KAIST, Daejeon 305-701 and [b] Department of Chemistry
and EHSRC, University of Ulsan, Ulsan 680-749, Republic of Korea

Contents

1. Experimental

General considerations. All operations were performed under an inert nitrogen atmosphere using standard Schlenk and glove box techniques. Anhydrous grade solvents (Aldrich) were dried by passing them through an activated alumina column and stored over activated molecular sieves (5Å). Spectrophotometric-grade solvents for photophysical measurements were used as received from Aldrich. Commercial reagents were used without any further purification after purchasing from Aldrich (Dimesitylboron fluoride (Mes_2BF), (4-bromophenylethynyl)trimethylsilane, *n*-tetrabutylammonium fluoride (TBAF), *n*-BuLi (2.5 M solution in *n*-hexane), potassium hydroxide, diethyl sulfide), and KatChem ($B_{10}H_{14}$, decaborane). (4-Ethynylphenyl)dimesitylborane (**1a**)[1] was analogously synthesized according to the reported procedures. Deuterated solvents from Cambridge Isotope Laboratories were used after drying over activated molecular sieves (5Å). NMR spectra of compounds were recorded on a Bruker Avance 400 spectrometer (400.13 MHz for ^1H, 100.62 MHz for ^{13}C, 128.38 MHz for ^{11}B) at ambient temperature. Chemical shifts are given in ppm, and are referenced against external Me_4Si (^1H, ^{13}C) and $BF_3{\cdot}Et_2O$ (^{11}B). Elemental analyses were performed on an EA1110 (Fisons Instruments) by Environmental Analysis Lab. at KAIST. HR FAB-MS measurement (JEOL JMS700) was carried out at Korea Basic Science Institute (Daegu).

Synthesis of 1-(Mes_2B)-4-(2-H-1,2-$C_2B_{10}H_{10}$)benzene (*closo*-1). This compound was prepared using an analogous method described previously.[2] To a toluene solution (50 mL) of decaborane ($B_{10}H_{14}$, 0.12 g, 1.02 mmol) and **1a** (0.30 g, 0.86 mmol) was added an excess amount of Et_2S (5 equiv) at room temperature. After heating to reflux, the reaction mixture was further stirred for 3 days. The solvent was removed under vacuum and the residue was re-dissolved in toluene (2 mL). The solution was purified by passing through an alumina column and the solvent was removed *in vacuo* affording *closo*-**1** as a white solid (0.29 g, 71%). ^1H NMR ($CDCl_3$): δ 7.42 (q, *J* = 6.7, 4H), 6.80 (s, 4H), 3.97 (br s, 1H), 3.30–1.50 (br, 10H), 2.28 (s, 6H), 1.94 (s, 12H). ^{13}C NMR ($CDCl_3$): δ 141.23, 140.74, 139.23, 136.38, 136.24, 128.33, 126.87, 77.20, 59.89, 23.42, 21.20 ^{11}B NMR ($CDCl_3$): δ 74.1, –2.0, –4.0, –8.8, –10.7, –12.7. HR FAB-MS: m/z Calcd for $[M–H]^+$ $C_{26}H_{36}B_{11}$, 469.3841; Found, 469.3845. Anal. Calcd for $C_{26}H_{37}B_{11}$: C, 66.60; H, 7.96. Found: C, 66.59; H, 8.05.

Synthesis of [NMe_4][1-(Mes_2B)-4-(2-H-1,2-$C_2B_9H_{10}$)benzene] ([NMe_4][*nido*-1]). *closo*-**1** (0.20 g, 0.42 mmol) was added into a solution of KOH (0.19 g, 3.40 mmol) in EtOH (8 mL). The mixture was stirred for 1 h at room temperature and then refluxed for 20 h. After cooling the mixture to room temperature, the solvent was evaporated and the resulting yellow residue was dissolved in water. Addition of excess NMe_4Cl in water gave a precipitate. The solid was filtered and dried *in vacuo* affording [NMe_4][*nido*-**1**] as a greenish white powder (0.19 g, 86%). Single crystals suitable for X-ray diffraction study were grown from vapor diffusion of Et_2O into a CH_2Cl_2 solution of *nido*-**1**. ^1H NMR ($CDCl_3$): δ 7.28 (d, *J* = 8.0, 2H), 7.17 (d, *J* = 8.0, 2H), 6.76 (s, 4H), 3.25 (s, 12H), 3.30–1.50 (br, 9H), 2.47 (br s, 1H), 2.26 (s, 6H), 1.96 (s, 12H), –2.39 (br s, 1H). ^{13}C NMR ($CDCl_3$): δ 149.60, 141.87, 140.71, 138.19, 136.33, 128.02, 125.88, 56.60, 56.56, 56.52, 23.46, 21.17. ^{11}B NMR (acetone-d_6): δ 72.6, –8.3, –9.8, –13.2, –15.6, –18.1, –19.0, –23.0, –32.4, –35.2. Anal. Calcd for $C_{30}H_{49}B_{10}N$: C, 67.75; H, 9.29; N, 2.63. Found: C, 67.89; H, 9.45; N, 2.63.

X-ray crystallography. A single crystal of [NMe_4][*nido*-**1**] of suitable size and quality was coated with Paratone oil and mounted onto a glass capillary. Reflection data were collected on a Bruker Apex II-CCD area detector diffractometer, with graphite-monochromated MoKa radiation ($\lambda = 0.71073$ Å). The hemisphere of reflection data were collected as ω scan frames with 0.3°/frame and an exposure time of 10 s/frame. Cell parameters were determined and refined by SMART program. Data reduction was performed using SAINT software. The data were corrected for Lorentz and polarization effects. An empirical absorption correction was applied using the SADABS program. The structure including the position of the bridging (B10–H–B7) and C–H101 hydrogen atoms was solved by direct methods and all nonhydrogen atoms were subjected to anisotropic refinement by full-matrix least-squares on F^2 by using the SHELXTL/PC package. All other hydrogen atoms were placed at their geometrically calculated positions and refined riding on the corresponding carbon and boron atoms with isotropic thermal parameters. The detailed crystallographic data are given in Table S1.

---

1. Z. An, S. A. Odom, R. F. Kelley, C. Huang, X. Zhang, S. Barlow, L. A. Padilha, J. Fu, S. Webster, D. J. Hagan, E. W. V. Stryland, M. R. Wasielewski and S. R. Marder, *J. Phys. Chem. A,* 2009, **113**, 5585.

2. W. Jiang, C. B. Knobler and F. Hawthorne, *Inorg. Chem.,* 1996, **35**, 3056.

Table S1. Crystallographic data and parameters for $[NMe_4]$**[***nido***-1]**

Compound	$[NMe_4]$**[***nido***-1]**$\cdot CH_2Cl_2$
formula	$C_{31}H_{51}B_{10}Cl_2N$
formula weight	616.73
crystal system	Triclinic
space group	P−1
a (Å)	8.5671(12)
b (Å)	11.2992(16)
c (Å)	22.491(3)
α (°)	96.168(6)
β (°)	97.986(6)
γ (°)	111.107(6)
V ($Å^3$)	1982.0(5)
Z	2
ρ_{calc} (g cm^{-3})	1.033
μ (mm^{-1})	0.185
F(000)	656
T (K)	100(2)
scan mode	*multi*
hkl range	–8 → +9, –12 → +12, –24 → +24
measd reflns	22273
unique reflns [R_{int}]	5264 [0.0452]
reflns used for refinement	5264
Refined parameters	415
R1[a] ($I > 2\sigma(I)$)	0.0804
wR2[b] all data	0.2634
GOF on F^2	1.073
ρ_{fin} (max/min) (e $Å^{-3}$)	0.631, –0.324

[a] $R1 = \sum||Fo| - |Fc||/\sum|Fo|$. [b] $wR2 = \{[\sum w(Fo2 - Fc2)2]/[\sum w(Fo2)2]\}^{1/2}$.

2. UV–vis absorption and fluorescence experiments.

UV–vis absorption and fluorescence spectra were recorded on a Jasco V-530 and a Spex Fluorog-3 Luminescence spectrophotometer, respectively. The measurements were performed in various solvents (hexane, toluene, acetone, DMSO, methanol, THF, and THF/H_2O (9/1 vol)) with a 1-cm quartz cuvette at ambient temperature unless otherwise stated. Quantum yields were measured with reference to that (Φ = 0.55) of quinine sulfate (0.5 M H_2SO_4) (W. H. Melhuish, *J. Phys. Chem.,* 1961, **65**, 229). Fluoride titration experiments were similarly performed with a 1-cm quartz cuvette. The detailed conditions are given in the figure captions in the main text and below.

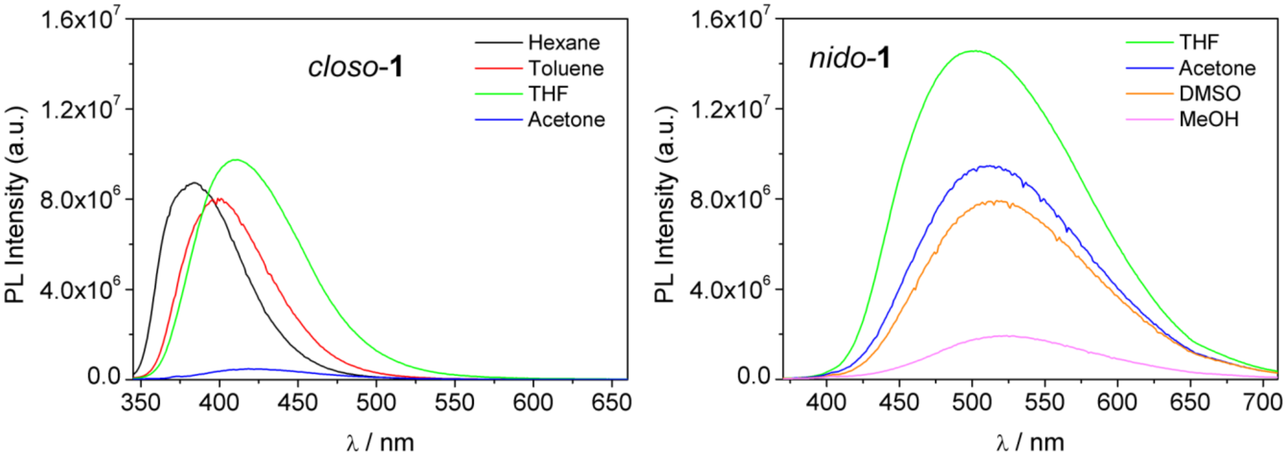

Figure S1. Fluorescence spectra of (left) *closo*-**1** (λ_{ex} = 335 nm) and (right) *nido*-**1** (λ_{ex} = 360 nm) in various solvents (5.0×10^{-5} M).

Table S2. UV–vis absorption and fluorescence data of *closo*-**1** and *nido*-**1**[a]

	closo-**1**			*nido*-**1**		
Solvent	λ_{abs}/nm (log ε)	λ_{em}/nm	Φ[b]	λ_{abs}/nm (log ε)	λ_{em}/nm	Φ[b]
Hexane	323 (3.78)	384	0.049	-	-	-
Toluene	323 (3.79)	399	0.053	-	-	-
THF	321 (4.09)	412	0.045	320 (4.19), 349 (4.23)	503	0.136
Acetone	332 (3.72)	419	0.004[c]	340 (4.06)	512	0.106
DMSO	-	-	-	336 (4.10)	517	0.013
Methanol	-	-	-	329 (4.17)	524	0.020

[a] Obtained using a 5.0×10^{-5} M solution. [b] Quinine sulfate (Φ = 0.55) was used as a standard.

[c] Corrected for the acetone emission at 402 nm under 335 nm excitation.

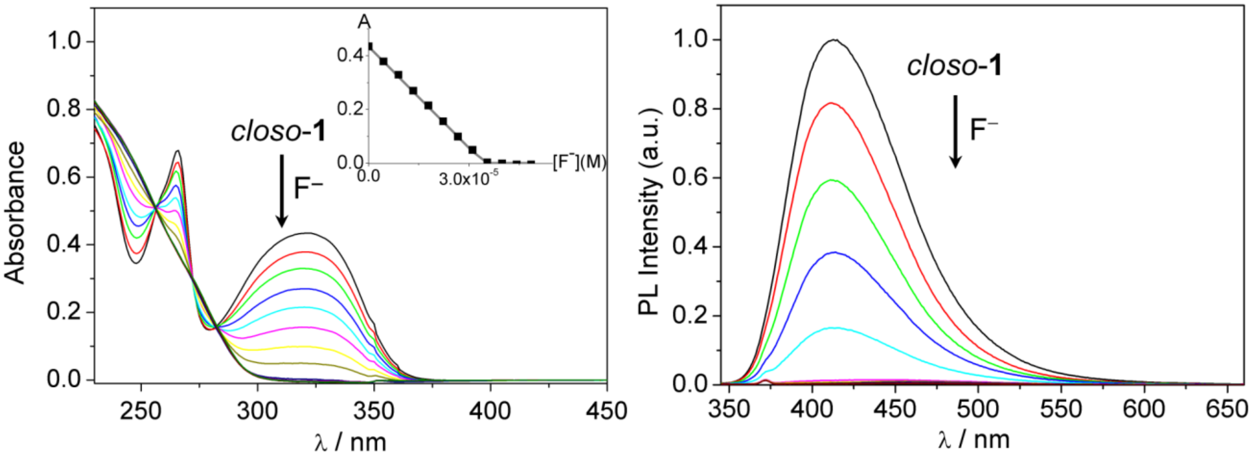

Figure S2. Spectral change in the (left) UV–vis absorption and (right) fluorescence of a solution of *closo*-**1** (3.5×10^{-5} M, $\lambda_{ex} = 335$ nm) in THF upon addition of TBAF ($0 - 4.9 \times 10^{-5}$ M for absorption and $0 - 6.9 \times 10^{-5}$ M for fluorescence). The inset shows the absorbance at 325 nm as a function of [F$^-$]. The line corresponds to the binding isotherm calculated with $K = 1.0 \times 10^9$ M^{-1}.

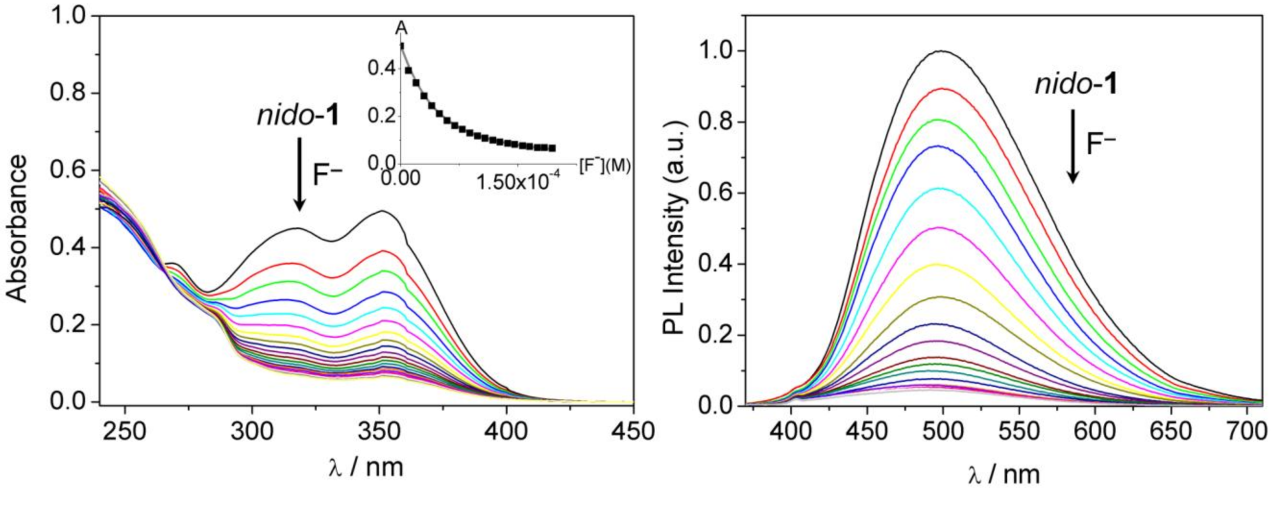

Figure S3. Spectral change in the (left) UV–vis absorption and (right) fluorescence of a solution of *nido*-**1** (3.0×10^{-5} M for absorption and 3.5×10^{-5} M for fluorescence, $\lambda_{ex} = 360$ nm) in THF upon addition of TBAF ($0 - 1.9 \times 10^{-4}$ M for absorption and $0 - 1.3 \times 10^{-4}$ M for fluorescence). The inset shows the absorbance at 351 nm as a function of [F$^-$]. The line corresponds to the binding isotherm calculated with $K = 4.1 \times 10^4$ M^{-1}.

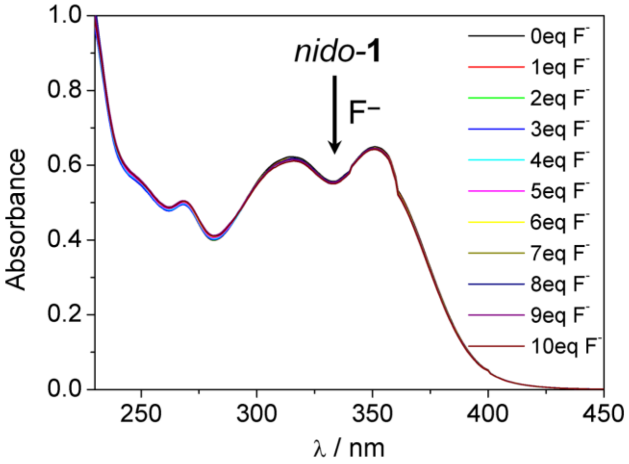

Figure S4. Spectral change in the UV−vis absorption of a solution of *nido*-**1** (4.5×10^{-5} M) in THF/H_2O (9:1 vol) upon addition of TBAF ($0 – 4.5 \times 10^{-4}$ M).

3. Computational details

The geometries of the ground state (S_0) of *closo*-**1** and *nido*-**1** were optimized using the density functional theory (DFT) method with the B3LYP functional and the 6-31G(d)[1] basis sets. The structures of the lowest-lying singlet excited (S_1) state were optimized using the configuration interaction single (CIS) with the 6-31G(d) basis sets. Time-dependent density functional theory (TD-DFT)[2] using the hybrid B3LYP functional (TD-B3LYP) was used with 6-31G(d) to obtain the electronic transition energies which include some account of electron correlation. The transition energy was calculated considering all the transition involved. To include the solvation effect of THF, the polarizable continuum model (PCM) was used in the calculations. All calculations described here were carried out using the GAUSSIAN 09 program[3].

---

1. J. S. Binkley, J. A. Pople and W. J. Hehre, *J. Am. Chem. Soc.*, 1980, **102**, 939.

2. E. Runge and E. K. Gross, *Phys. Rev. Lett.* 1984, **52**, 997.

3. Gaussian 09, Revision A.02, M. J. Frisch, G. W. Trucks, H. B. Schlegel, G. E. Scuseria, M. A. Robb, J. R. Cheeseman, J. A. Montgomery, Jr., T. Vreven, K. N. Kudin, J. C. Burant, J. M. Millam, S. S. Iyengar, J. Tomasi, V. Barone, B. Mennucci, M. Cossi, G. Scalmani, N. Rega, G. A. Petersson, H. Nakatsuji, M. Hada, M. Ehara, K. Toyota, R. Fukuda, J. Hasegawa, M. Ishida, T. Nakajima, Y. Honda, O. Kitao, H. Nakai, M. Klene, X. Li, J. E. Knox, H. P. Hratchian, J. B. Cross, V. Bakken, C. Adamo, J. Jaramillo, R. Gomperts, R. E. Stratmann, O. Yazyev, A. J. Austin, R. Cammi, C. Pomelli, J. W. Ochterski, P. Y. Ayala, K. Morokuma, G. A. Voth, P. Salvador, J. J. Dannenberg, V. G. Zakrzewski, S. Dapprich, A. D. Daniels, M. C. Strain, O. Farkas, D. K. Malick, A. D. Rabuck, K. Raghavachari, J. B. Foresman, J. V. Ortiz, Q. Cui, A. G. Baboul, S. Clifford, J. Cioslowski, B. B. Stefanov, G. Liu, A. Liashenko, P. Piskorz, I. Komaromi, R. L. Martin, D. J. Fox, T. Keith, M. A. Al-Laham, C. Y. Peng, A. Nanayakkara, M. Challacombe, P. M. W. Gill, B. Johnson, W. Chen, M. W. Wong, C. Gonzalez and J. A. Pople, Gaussian, Inc., Wallingford CT, 2009.

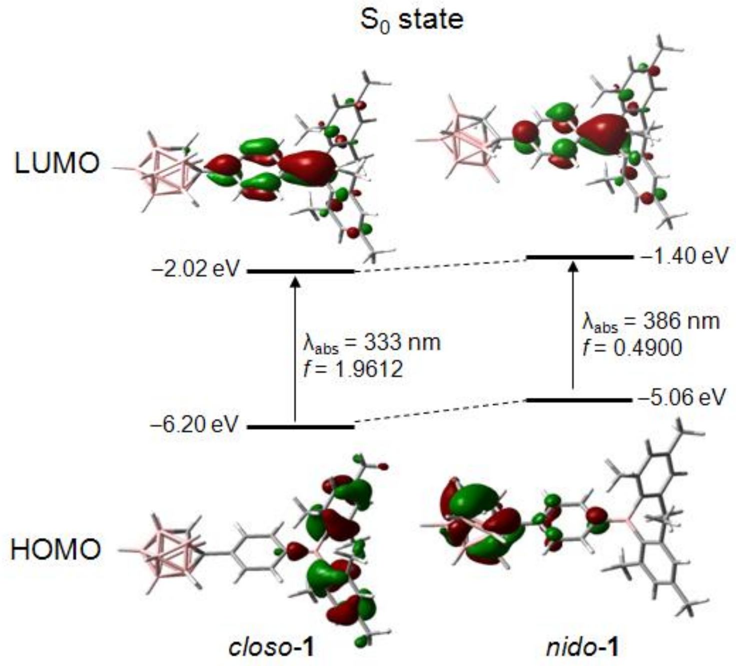

Figure S5. Molecular orbital diagrams of HOMO and LUMO for *closo*-**1** and *nido*-**1** at their lowest singlet state (S$_0$) with their relative energies from DFT calculation. The transition energy (in nm) was calculated using the TD-B3LYP method with 6-31G(d) basis sets.

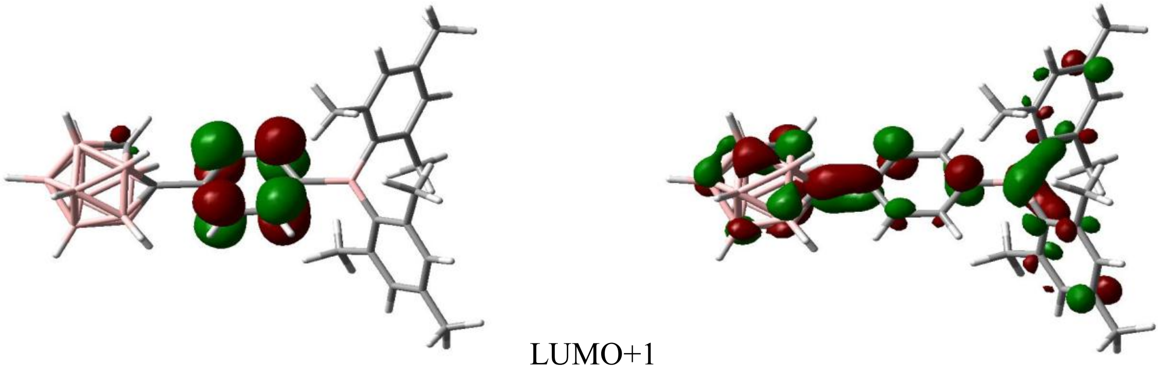

LUMO+2 LUMO+1

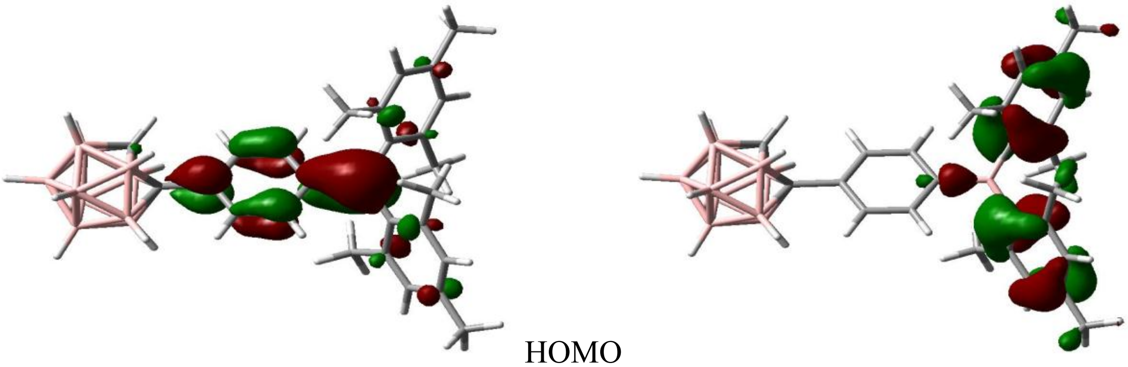

LUMO HOMO

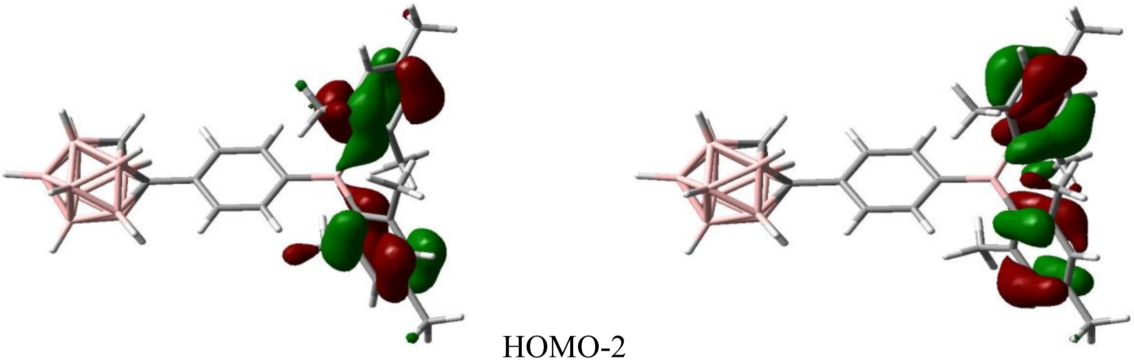

HOMO-1 HOMO-2

Figure S6. Frontier molecular orbitals of *closo*-**1** from B3LYP calculations at the lowest singlet state (S_0) (Isovalue = 0.04 a.u.).

Table S3. Computed absorption wavelength (λ_{calc} in nm) and oscillator strength ($f_{calc.}$) for *closo*-**1** from TD-B3LYP calculations using the B3LYP geometries at their lowest singlet state (S_0) fully optimized geometries.

state	$\lambda_{calc.}$	$f_{calc.}$	major contribution
1	333.08	1.9621	HOMO → LUMO (61.63%)
2	348.17	0.0794	$HOMO_{-1}$ → LUMO(96.79%)
3	340.25	0.0787	$HOMO_{-2}$ → LUMO(96.94%)
4	335.19	0.0190	$HOMO_{-3}$ → LUMO(98.30%)
5	276.97	0.0188	$HOMO_{-5}$ → LUMO(87.59%)
6	273.38	0.4291	$HOMO_{-4}$ → LUMO(89.63%)
7	270.64	0.0488	HOMO → $LUMO_{+1}$(82.06%)
8	266.97	0.0121	HOMO → $LUMO_{+2}$(31.31%) $HOMO_{-1}$ → $LUMO_{+1}$(29.24%)

Table S4. Molecular orbital distributions (in %) of *closo*-**1** at their lowest singlet state (S_0) fully optimized geometries.

molecular orbital	Mesityl 1	Mesityl 2	Boron	Carborane	Phenyl
$LUMO_{+2}$	5.8	5.6	5.0	18.9	64.7
$LUMO_{+1}$	13.1	16.1	5.4	44.5	20.9
LUMO	12.1	16.1	23.9	11.9	36.0
HOMO	42.5	44.7	1.3	0.0	11.5
$HOMO_{-1}$	51.1	44.2	1.4	0.3	3.1
$HOMO_{-2}$	55.6	40.6	1.1	0.3	2.4

Table S5. Molecular orbital energies (in eV) of *closo*-**1** from B3LYP calculations at their lowest singlet state (S_0) fully optimized geometries.

MO	$HOMO_{-2}$	$HOMO_{-1}$	HOMO	LUMO	$LUMO_{+1}$	$LUMO_{+2}$
Energy	-6.33	-6.28	-6.20	-2.02	-0.64	-0.58

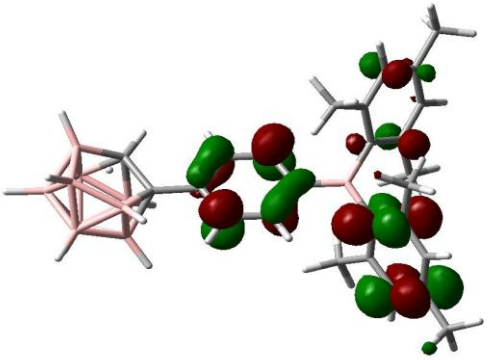

LUMO+2

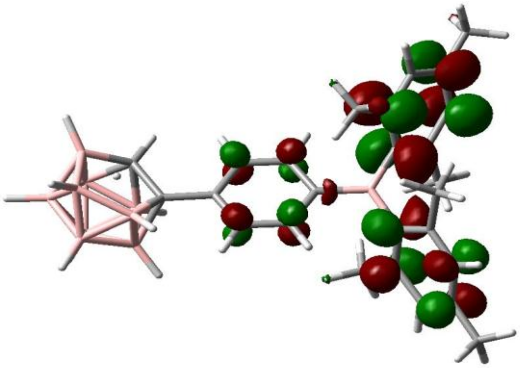

LUMO+1

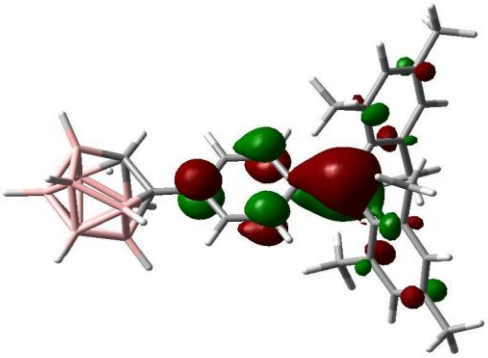

LUMO

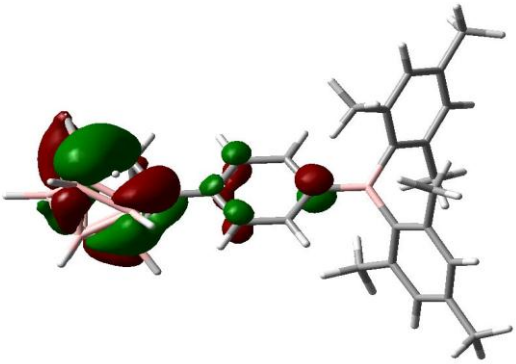

HOMO

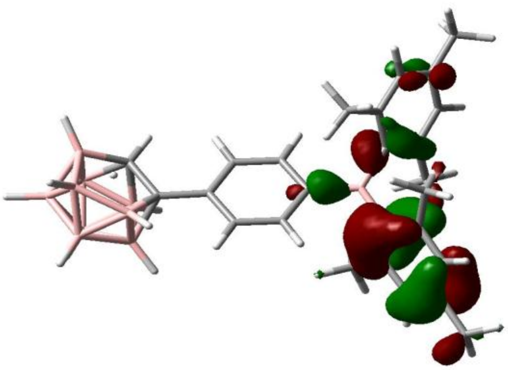

HOMO-1

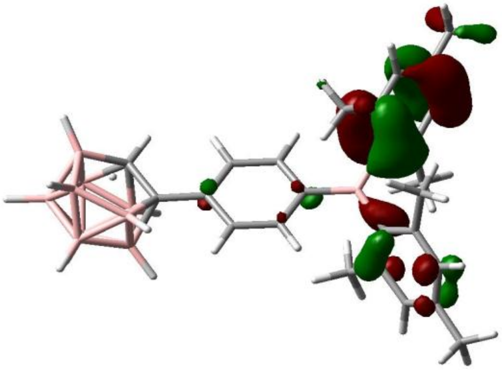

HOMO-2

Figure S7. Frontier molecular orbitals of *nido*-**1** from B3LYP calculations at the lowest singlet state (S_0) (Isovalue = 0.04 a.u.).

Table S6. Computed absorption wavelength (λ_{calc} in nm) and oscillator strength ($f_{calc.}$) for *nido*-**1** from TD-B3LYP calculations using the B3LYP geometries at their lowest singlet state (S_0) fully optimized geometries.

state	$\lambda_{calc.}$	$f_{calc.}$	major contribution
1	386.46	0.4900	HOMO → LUMO(98.05%)
2	335.76	0.0913	$HOMO_{-1}$ → LUMO(89.05%)
3	325.75	0.0409	$HOMO_{-2}$ → LUMO(87.49%)
4	317.92	0.0275	$HOMO_{-3}$ → LUMO(97.30%)
5	309.35	0.0136	$HOMO_{-4}$ → LUMO(98.13%)
6	276.41	0.2632	$HOMO_{-5}$ → LUMO(91.80%)
7	261.18	0.0156	HOMO → $LUMO_{+1}$(44.04%) HOMO → $LUMO_{+2}$(31.23%) $HOMO_{-6}$ → LUMO(10.43%)

Table S7. Molecular orbital distributions (in %) of *nido*-**1** at their lowest singlet state (S_0) fully optimized geometries.

molecular orbital	Mesityl 1	Mesityl 2	Boron	Carborane	Phenyl
$LUMO_{+2}$	16.2	45.0	2.7	4.3	31.8
$LUMO_{+1}$	43.4	25.5	7.7	1.3	22.2
LUMO	14.8	19.5	26.6	8.4	30.6
HOMO	1.3	1.1	1.0	81.9	14.7
$HOMO_{-1}$	19.6	66.9	1.5	0.8	11.2
$HOMO_{-2}$	68.4	18.5	1.2	4.0	7.9

Table S8. Molecular orbital energies (in eV) of *nido*-**1** from B3LYP calculations at their lowest singlet state (S_0) fully optimized geometries.

MO	$HOMO_{-2}$	$HOMO_{-1}$	HOMO	LUMO	$LUMO_{+1}$	$LUMO_{+2}$
Energy	-5.92	-5.89	-5.06	-1.40	0.17	0.24

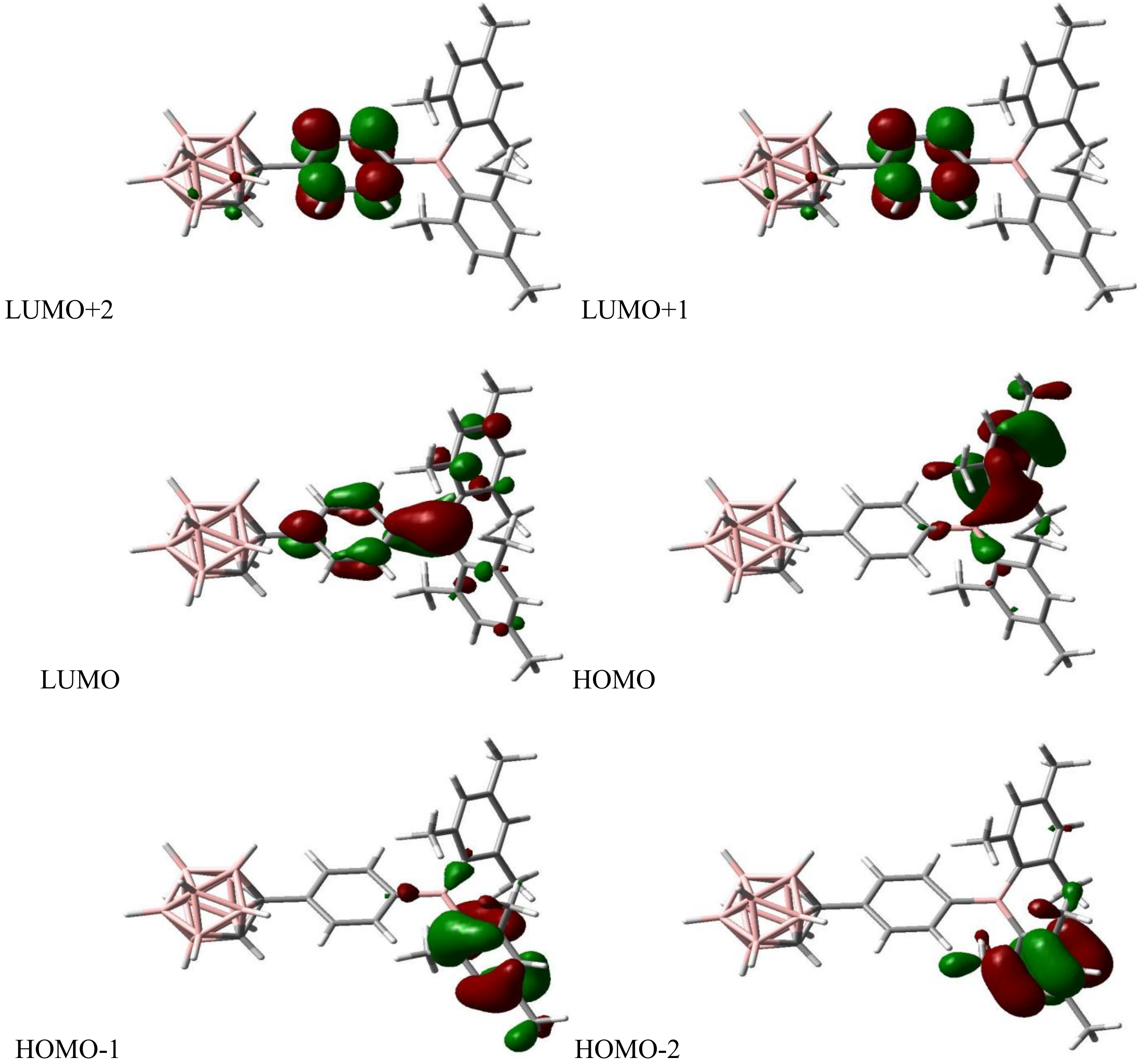

LUMO+2 LUMO+1

LUMO HOMO

HOMO-1 HOMO-2

Figure S8. Frontier molecular orbitals of *closo*-**1** from B3LYP calculations at the first excited singlet state (S_1) (Isovalue = 0.04 a.u.).

Table S9. Computed emission wavelength (λ_{calc} in nm) and oscillator strength ($f_{calc.}$) for *closo*-**1** from TD-B3LYP calculations using the CIS geometries at their first excited singlet state (S_1) fully optimized geometries.

state	$\lambda_{calc.}$	$f_{calc.}$	major contribution
1	400.29	0.1751	HOMO → LUMO(98.19%)

Table S10. Molecular orbital distributions (in %) of *closo*-**1** at their first excited singlet state (S_1) fully optimized geometries.

molecular orbital	Mesityl 1	Mesityl 2	Boron	Carborane	Phenyl
$LUMO_{+2}$	3.7	3.9	3.6	22.5	66.2
$LUMO_{+1}$	6.1	28.7	3.4	36.1	25.7
LUMO	13.1	22.4	23.6	9.6	31.3
HOMO	9.8	78.9	2.7	0.5	8.1
$HOMO_{-1}$	84.9	6.3	1.6	0.2	6.9
$HOMO_{-2}$	95.0	4.0	0.3	0.0	0.7

Table S11. Molecular orbital energies (in eV) of *closo*-**1** from B3LYP calculations at their first excited singlet state (S_1) fully optimized geometries.

MO	$HOMO_{-2}$	$HOMO_{-1}$	HOMO	LUMO	$LUMO_{+1}$	$LUMO_{+2}$
Energy	-6.34	-6.22	-5.92	-2.12	-0.76	-0.47

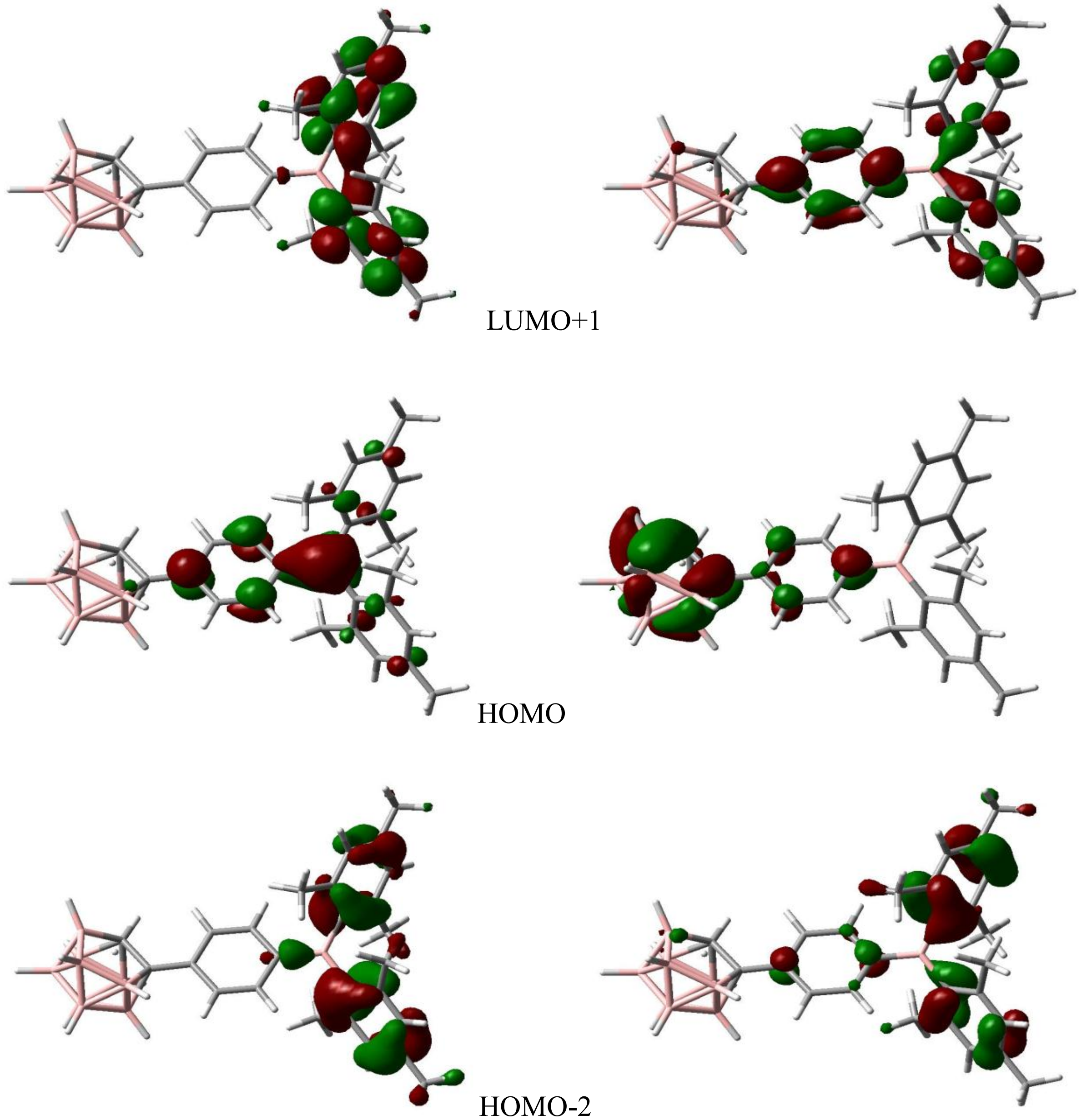

LUMO+2 LUMO+1

LUMO HOMO

HOMO-1 HOMO-2

Figure S9. Frontier molecular orbitals of *nido*-**1** from B3LYP calculations at the first excited singlet state (S_1) (Isovalue = 0.04 a.u.).

Table S12. Computed emission wavelength (λ_{calc} in nm) and oscillator strength ($f_{calc.}$) for *nido*-**1** from TD-B3LYP calculations using the CIS geometries at their first excited singlet state (S_1) fully optimized geometries.

state	$\lambda_{calc.}$	$f_{calc.}$	major contribution
1	432.18	0.6452	HOMO → LUMO(98.68%)

Table S13. Molecular orbital distributions (in %) of *nido*-**1** at their first excited singlet state (S_1) fully optimized geometries.

molecular orbital	Mesityl 1	Mesityl 2	Boron	Carborane	Phenyl
LUMO_{+2}	45.0	41.4	3.9	0.1	9.5
LUMO_{+1}	24.1	27.9	1.7	13.9	32.4
LUMO	17.5	17.3	24.1	11.1	29.9
HOMO	1.4	1.5	1.4	77.8	17.8
HOMO_{-1}	34.3	53.7	1.3	0.3	10.4
HOMO_{-2}	49.0	28.4	1.1	8.7	12.9

Table S14. Molecular orbital energies (in eV) of **1**-*nido* from B3LYP calculations at their first excited singlet state (S_1) fully optimized geometries.

MO	HOMO_{-2}	HOMO_{-1}	HOMO	LUMO	LUMO_{+1}	LUMO_{+2}
Energy	-5.88	-5.87	-4.74	-1.47	0.21	0.27

Table S15. Cartesian coordinates of *closo*-**1** from B3LYP calculation at the lowest singlet state (S_0) (in Å).

	X	Y	Z
C	1.601684	2.167362	2.182201
C	4.028819	-0.61489	2.148074
C	-4.81481	1.292953	0.026115
C	4.353237	-2.86539	1.123686
C	3.69541	-1.63432	1.076746
C	-3.99554	-0.13433	0.010677
C	2.431585	2.406345	0.935202
C	-1.74948	-1.14359	0.571326
C	3.04567	3.661295	0.820203
C	-0.35746	-1.11732	0.55765
C	-2.48507	-0.08809	0.013894
C	4.837866	-5.19474	0.259357
C	0.365978	-0.03462	0.019518
C	4.117101	-3.87006	0.18067
C	-1.78474	0.990417	-0.54649
C	2.727321	-1.37796	0.065319
C	2.667897	1.401646	-0.03783
C	-0.39303	1.02024	-0.52438
C	3.892354	3.975841	-0.23947
C	4.531105	5.338757	-0.36328
C	3.186161	-3.60845	-0.8242
C	2.481517	-2.40043	-0.88919
C	3.551264	1.715643	-1.11185
C	4.130015	2.982372	-1.19649
C	1.490194	-2.24447	-2.02936
C	3.864319	0.721925	-2.21288
H	-6.60042	2.188584	1.500752
H	-6.88988	-0.76997	2.462945
H	2.253026	2.007164	3.051984
H	4.769924	-1.01731	2.845871
H	3.147043	-0.3341	2.736467
H	0.975828	3.037728	2.410972
H	-8.45051	0.16296	-0.02052
H	-4.3236	-2.14498	1.480235
H	0.946779	1.298169	2.101886
H	4.434822	0.306977	1.719792
H	-4.19812	2.181789	0.052278
H	5.079568	-3.04276	1.915017
H	2.855724	4.409652	1.588249
H	-2.26431	-1.9909	1.008249
H	4.392539	-5.84389	1.025213
H	-6.57369	2.223964	-1.45986
H	-6.9818	-2.5419	-0.03867
H	0.185632	-1.95713	0.982708
H	4.340277	5.952699	0.52259
H	5.892864	-5.06245	0.525199
H	-2.318	1.811541	-1.01514
H	4.792505	-5.73339	-0.6927
H	0.119635	1.878806	-0.9489
H	5.617533	5.261267	-0.49209
H	-6.85164	-0.70414	-2.50069
H	-4.10616	0.783155	-2.31913
H	4.144291	5.882864	-1.2347
H	-4.25727	-2.10149	-1.49579
H	3.000058	-4.36592	-1.58388
H	0.490519	-2.59415	-1.74393
H	4.270896	-0.21319	-1.81657
H	4.788031	3.203263	-2.03536
H	1.378902	-1.2094	-2.36187
H	2.971974	0.461763	-2.79631
H	1.806723	-2.83779	-2.89396
H	4.595475	1.13907	-2.91247
B	-6.26907	1.220431	0.902901
B	-6.36713	-0.46931	1.440278
B	-7.26681	0.069422	-0.01169
B	-4.902	-1.30576	0.879859
B	-6.25123	1.242883	-0.87838
B	-6.41658	-1.49749	-0.02468
B	-6.34433	-0.43598	-1.46129
B	1.944094	-0.00473	0.02213
B	-4.79378	0.397976	-1.43924
B	-4.88314	-1.29063	-0.90069
B	-4.81399	0.366141	1.46696
H	-4.13154	0.731692	2.36007

Table S16. Cartesian coordinates of *nido*-**1** from B3LYP calculation at the lowest singlet state (S_0) (in Å).

	X	Y	Z
C	-1.64223	-2.17163	2.215136
C	-3.78769	0.702324	2.225847
C	4.942679	-1.30146	-0.27751
C	-4.16461	2.916722	1.139751
C	-3.50136	1.686088	1.109322
C	4.125628	-0.01424	0.095994
C	-2.46829	-2.36959	0.95747
C	1.901411	1.094732	0.486365
C	-3.16845	-3.58189	0.855908
C	0.515956	1.104628	0.470011
C	2.637818	-0.03648	0.065559
C	-4.67471	5.221666	0.220823
C	-0.24733	-0.01499	0.053192
C	-3.96129	3.890979	0.160113
C	1.889339	-1.15726	-0.35241
C	-2.5712	1.392719	0.07652
C	-2.59516	-1.38083	-0.05073
C	0.501269	-1.14689	-0.34676
C	-3.99593	-3.87213	-0.22422
C	-4.72711	-5.19043	-0.32923
C	-3.05831	3.599422	-0.86176
C	-2.3536	2.389428	-0.9119
C	-3.44817	-1.67748	-1.15226
C	-4.11932	-2.89924	-1.22211
C	-1.3748	2.209738	-2.05842
C	-3.6218	-0.71246	-2.30701
H	6.720812	-2.64666	0.740977
H	7.129766	-0.03536	2.630539
H	-2.29437	-2.04494	3.090349
H	-4.50944	1.119584	2.936427
H	-2.88065	0.452305	2.788956
H	5.300766	-0.36505	1.930987
H	-1.01365	-3.0488	2.410399
H	8.534637	-0.21444	0.076053
H	4.335821	1.471099	2.093692
H	-0.98535	-1.3034	2.158945
H	-4.19474	-0.23931	1.843362
H	4.353901	-2.1608	-0.57951
H	-4.86455	3.116639	1.950041
H	-3.05579	-4.31793	1.651521
H	2.440774	1.9719	0.825354
H	-4.11807	5.947383	0.830327
H	6.727639	-1.68471	-2.07681
H	7.026676	2.3367	0.864573
H	-0.0039	2.001479	0.799586
H	-4.61342	-5.78365	0.584503
H	-5.67141	5.123795	0.666983
H	2.399669	-2.05163	-0.69191
H	-4.79165	5.660313	-0.7766
H	-0.02804	-2.03874	-0.67448
H	-5.80094	-5.04322	-0.50268
H	6.980115	1.43178	-2.02811
H	4.237238	-0.10096	-2.42807
H	-4.34905	-5.79459	-1.16488
H	4.36232	2.36856	-0.69757
H	-2.88758	4.336721	-1.64529
H	-0.35952	2.499927	-1.76438
H	-3.89923	0.289285	-1.96651
H	-4.75536	-3.10028	-2.08374
H	-1.30988	1.175644	-2.40486
H	-2.69548	-0.61004	-2.88686
H	-1.66382	2.834699	-2.91108
H	-4.39712	-1.06499	-2.99592
B	6.329823	-1.53972	0.505226
B	6.504007	-0.10802	1.613548
B	7.339997	-0.18255	0.043077
B	4.925996	0.805768	1.296858
B	6.375407	-0.97853	-1.18171
B	6.460963	1.329814	0.557476
B	6.444859	0.800739	-1.16787
B	-1.79474	-0.00091	0.029535
B	4.911298	-0.03418	-1.45039
B	4.981657	1.39218	-0.40986

Table S17. Cartesian coordinates of *closo*-**1** from CIS calculation at the first excited singlet state (S_1) (in Å).

	X	Y	Z
C	1.558153	-2.0947	-2.11074
C	4.520882	0.556274	-1.66444
C	-4.77173	-1.36324	-0.01289
C	4.30302	2.93491	-1.02966
C	3.888138	1.651378	-0.85053
C	-3.98837	0.061817	-0.02506
C	2.485215	-2.34208	-0.93625
C	-1.75969	1.138002	-0.49823
C	3.144105	-3.56391	-0.90142
C	-0.37957	1.142392	-0.4796
C	-2.47721	0.048885	-0.01191
C	4.218709	5.419151	-0.5981
C	0.377776	0.066996	0.022097
C	3.740561	4.026625	-0.31294
C	-1.75192	-1.02702	0.50153
C	2.770562	1.373983	0.049313
C	2.708665	-1.38346	0.07522
C	-0.37344	-1.02065	0.504857
C	4.02421	-3.89831	0.115458
C	4.703557	-5.24722	0.144882
C	2.799797	3.76413	0.673233
C	2.382225	2.478137	0.95017
C	3.604367	-1.7251	1.105779
C	4.242681	-2.96041	1.109232
C	1.476114	2.242729	2.118689
C	3.891443	-0.7904	2.262119
H	-6.52252	-2.349	-1.47019
H	-6.87241	0.583353	-2.51959
H	1.831269	-2.72786	-2.94777
H	5.28074	0.964953	-2.31939
H	3.776293	0.052945	-2.27133
H	0.526948	-2.31542	-1.85587
H	-8.43544	-0.31903	-0.02061
H	-4.33807	2.032485	-1.54704
H	1.585622	-1.06584	-2.44711
H	4.976593	-0.1997	-1.03727
H	-4.15084	-2.23429	-0.0132
H	5.074714	3.14521	-1.74893
H	2.972645	-4.26954	-1.69747
H	-2.27488	1.990791	-0.8939
H	3.985276	5.700096	-1.62313
H	-6.51743	-2.31013	1.477708
H	-7.02192	2.414105	-0.06
H	0.125675	2.006474	-0.87325
H	4.965678	-5.57865	-0.85436
H	5.29855	5.487197	-0.49021
H	-2.25491	-1.87689	0.923882
H	3.761647	6.143695	0.063686
H	0.139884	-1.87453	0.907045
H	5.611112	-5.21958	0.737602
H	-6.87357	0.642293	2.452787
H	-4.09215	-0.79598	2.320011
H	4.052067	-6.00215	0.57765
H	-4.29476	2.06633	1.424583
H	2.427538	4.578663	1.269501
H	0.432732	2.19776	1.81292
H	4.251889	0.178308	1.930239
H	4.922667	-3.19453	1.910796
H	1.693439	1.295184	2.59793
H	3.000809	-0.61738	2.857834
H	1.576568	3.041939	2.844272
H	4.645386	-1.21032	2.918208
B	-6.22331	-1.35876	-0.90288
B	-6.35224	0.31808	-1.49115
B	-7.25823	-0.20403	-0.02288
B	-4.90314	1.201867	-0.93403
B	-6.21839	-1.33656	0.882034
B	-6.4351	1.386895	-0.04314
B	-6.35219	0.358551	1.429863
B	1.952764	0.047427	0.03679
B	-4.77825	-0.44471	1.433243
B	-4.8984	1.231441	0.851021
B	-4.77636	-0.48681	-1.47726
H	-4.08216	-0.86139	-2.34894

Table S18. Cartesian coordinates of *nido*-**1** from CIS calculation at the first excited singlet state (S_1) (in Å).

	X	Y	Z
C	-1.32519	-2.33562	1.968771
C	-3.90405	0.601168	2.112908
C	4.933916	-1.16239	-0.61217
C	-4.21976	2.848635	1.124539
C	-3.55568	1.635564	1.061365
C	4.115472	0.006493	-0.022
C	-2.34139	-2.44474	0.849096
C	1.910861	1.087577	0.469338
C	-3.05039	-3.64184	0.770051
C	0.55229	1.09477	0.46441
C	2.66894	-0.02631	-0.02248
C	-4.70826	5.187012	0.316063
C	-0.23429	-0.01074	-0.00975
C	-3.96865	3.873318	0.220443
C	1.901879	-1.14128	-0.47979
C	-2.56997	1.393672	0.070448
C	-2.58272	-1.39837	-0.06557
C	0.541762	-1.12984	-0.47896
C	-4.00762	-3.86415	-0.1992
C	-4.76365	-5.16921	-0.28436
C	-3.02185	3.643197	-0.7571
C	-2.32555	2.439181	-0.84428
C	-3.57854	-1.63231	-1.04817
C	-4.25527	-2.83877	-1.10353
C	-1.32086	2.32341	-1.97409
C	-3.92455	-0.59613	-2.09872
H	6.554829	-2.77461	0.275563
H	6.936435	-0.64711	2.680804
H	-1.59817	-2.9872	2.793452
H	-4.56573	1.027495	2.860096
H	-3.01858	0.24163	2.624468
H	5.151424	-0.69156	1.812132
H	-0.33443	-2.62878	1.634907
H	8.516528	-0.35422	0.254739
H	4.237923	1.076755	2.289661
H	-1.24042	-1.3269	2.349133
H	-4.39778	-0.26207	1.68335
H	4.368765	-1.91637	-1.12247
H	-4.95117	3.005067	1.901155
H	-2.84568	-4.41471	1.492925
H	2.437856	1.940939	0.849027
H	-4.46832	5.708356	1.23957
H	6.848285	-1.26995	-2.29029
H	7.029128	2.087247	1.405966
H	0.039888	1.956938	0.850881
H	-4.48799	-5.83785	0.523933
H	-5.78473	5.037616	0.301546
H	2.402017	-2.02004	-0.83728
H	-4.45327	5.843819	-0.50855
H	0.018666	-1.99161	-0.85184
H	-5.83748	-5.00919	-0.23138
H	7.164092	1.795357	-1.56489
H	4.446665	0.475045	-2.5048
H	-4.56096	-5.68237	-1.22122
H	4.45702	2.489216	-0.22445
H	-2.81507	4.415449	-1.48002
H	-0.32733	2.620935	-1.65328
H	-4.4084	0.271569	-1.66691
H	-4.99433	-2.98935	-1.87407
H	-1.23873	1.312357	-2.34855
H	-3.03918	-0.24417	-2.61575
H	-1.60434	2.968826	-2.80016
H	-4.5943	-1.01754	-2.84153
B	6.246144	-1.627	0.215557
B	6.396595	-0.44359	1.64187
B	7.338508	-0.25139	0.134756
B	4.888345	0.573889	1.438609
B	6.4499	-0.72582	-1.31421
B	6.469968	1.176865	0.885114
B	6.557686	1.010156	-0.91292
B	-1.77962	-0.00578	-0.0013
B	5.040801	0.306164	-1.49827
B	5.02278	1.453914	-0.13911